

Detection and Classification of Alopecia Areata Using Diverse Feature-Set

Amna Noreen¹, Haider Ali Khan¹, Syed M. Adnan¹, Wakeel Ahmed¹, Syed Haseeb Amjad¹,

¹Department of Computer Science, University of Engineering and Technology, Taxila, Pakistan.

ARTICLE INFO

Article History:

Received:	April	14, 2025
Revised:	June	25, 2025
Accepted:	June	26, 2025
Available Online:	June	27, 2025

Keywords:

Alopecia Areata
Color Histogram
Computer Vision
Classification
Haralick

Classification Codes:

Funding:

This research received no specific grant from any funding agency in the public or not-for-profit sector.



ABSTRACT

Alopecia Areata is a well-known autoimmune disorder characterized by hair loss on the scalp and other parts of the body, affecting millions of people around the world. This condition can greatly affect a person's psychological well-being and self-esteem, emphasizing the significance of early detection for better disease management and possible regrowth of hair. This study uses computer vision techniques to propose a comprehensive method for detecting alopecia areata from camera images. Two different datasets of images are used: Dermnet for alopecia areata images and Figaro1k for the images of healthy hair and employed with a preprocessing phase that involves histogram equalization to enhance image quality. Subsequently, to maximize the dataset's power, features related to color, texture, and shape are extracted from images, along with feature fusion and selection. Many renowned classifiers, such as SVM, Random Forest, Decision Tree, Naive Bayes, Logistic Regression, KNN, and ANN, are applied to detect the effectiveness of the model. ANN is applied with a batch size of 64 and four layers. The proposed techniques gain an accuracy of 96.43, surpassing the related research methods. With the use of modern computer vision and machine learning methods, this study holds promise of improving the early detection and treatment of Alopecia Areata and can enhance patient outcomes.

© 2025 The authors published by JCIS. This is an Open Access Article under the Creative Common Attribution Non-Commercial 4.0

Corresponding Author's Email: haider.khan@students.uettaxila.edu.pk

1. Introduction

Alopecia Areata is an autoimmune disorder that causes hair loss and has an impact on millions of people globally [1]. The initial symptoms involve spots of hair loss, which can lead to complete baldness of the scalp (Alopecia Totalis) or even complete body hair loss (Alopecia Universalis), if it is not identified early [2] [3]. Figure 1 illustrates the severity of Alopecia Areata. Therefore, timely and precise identification is required for effective treatment and management [3] [4].

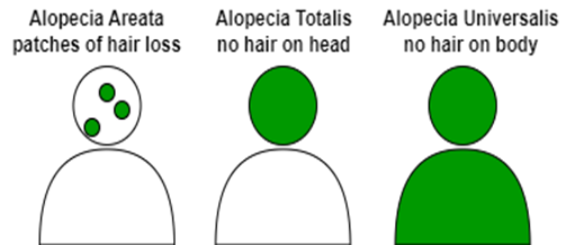


Figure 1: Categories of Alopecia Areata [5]

The traditional approaches for diagnosing Alopecia Areata (AA) primarily depend on clinical evaluations, which can be subjective and less accurate [4]. Recently, there has been an increasing focus on using the systems of computer-aided diagnosis (CAD) to increase the accuracy and fairness of Alopecia identification and classification. These systems analyze the images of hair loss for identifying the typical Alopecia features, consisting of shapes, color, and textures, which are then used for classifying the hair conditions [6].

Dermoscopy is the predominant method used for identifying Alopecia Areata, utilizing a dermatoscope to closely examine skin lesions and the scalp [7]. Although this technique is effective, it has limitations, such as the need for specialized equipment, which can restrict accessibility. Furthermore, analyzing the dermoscopic images requires expertise, and other factors such as angle and lighting for an impactful diagnostic. In contrast, employing standard camera images for detection presents notable benefits; these images are more accessible and easier to obtain using common devices like smartphones and webcams. Moreover, camera technology is generally more cost-effective, thereby allowing for wider application in various clinical and residential environments. This user-friendly approach enables real-time tracking of changes in scalp and hair conditions, facilitating frequent assessments without specialized tools [8].

The rest of the paper is divided into the following sections. Related work is described in the Literature Review section. The Materials and Methods section narrates the datasets used in this research and the proposed methodology in detail. Results obtained by using the proposed methodology and different comparisons are given in the Results and Discussion section. Finally, the Conclusion and Future Work is given in the last section Conclusion and Future Work.

1.1 Literature Review

Visual examination, often supplemented by microscopic techniques, serves as a widespread method for diagnosing hair loss, evaluating its severity, and recognizing additional scalp disorders. Alopecia Areata has been the focus of traditional machine learning and deep learning techniques. Olsen and Canfield employed the Severity of Alopecia Tool (SALT) to assess hair density and the proportion of hair loss by measuring the hair loss in each scalp quadrant and aggregating these percentages to calculate the overall hair loss on the scalp [9]. This complicated scoring system can make it challenging to ensure consistent reliability; retaining uniformity is important for tracking the progression of disease and effectiveness of the treatment. In order to enhance this, the 100 images from young patients of Alopecia Areata were marked by a hair specialist, classifying the disease in distinct ways, like normal density, clinically affected scalp, low-density hair patches, and hair partition.

Bernardis and Castelo-Soccio developed an algorithm to distinguish between bald and normal scalp regions, as well as to identify areas with low hair density [10]. Lee et al. introduced the AloNet deep learning architecture for measuring Alopecia Areata, training it on a dataset of 2000 images annotated by a dermatologist and achieving an accuracy of 77.42% with AlexNet and 75% with VGG19 when assessed by eight dermatologists [11]. Kapoor and Mishra employed feedforward and backpropagation neural networks to diagnose Alopecia Areata early, achieving 91.00% accuracy [12]. Seo and Park suggested using grid line selection and eigenvalues to process scalp images for hair loss information via Trichoscopy [13].

Table 1: Summary of the State-of-the-Art Techniques

Ref	Year	Dataset	Feature Extraction Technique	Classifier	Acc (%)
[6]	2021	Dermnet, Figaro1k	Shape, Color, and Texture feature	SVM	91.40
[14]	2022	Dermnet, Figaro1k	CNN	CNN	92.00
[15]	2023	Dermnet	FRCNN	FRCNN	84.30
[1]	2023	Dermnet	Shape, color, and texture features	MELM	92.64

As far as female pattern hair loss (FPHL) is concerned, it is typically diagnosed by eye inspection and the Ludwig and Savin scales, Hung et al. developed a method to assess the balding area using Principal Component Analysis on images of 33 women with FPHL, showing a strong association between Balding Width (BW) and hair loss grades on the Savin scale [16],[17],[18]. Lee and Yang captured crown pictures using webcam and microscope camera sensors, extracting binary images with the Otsu threshold value and applying the K-means clustering algorithm twice (with $k=4$ and $k=2$) to segment the image into background, hair, and non-hair components, achieving an accuracy of 51.00-95.00% using the Hamilton-Norwood scale [19],[20]. Benhabiles et al. classified 675 images for male pattern baldness in facial photographs, achieving an average accuracy of 82.00-86.00% using the Hamilton-Norwood scale [21].

Shakeel et al. (2021) proposed a method for detecting and classifying Alopecia Areata from camera images. For image enhancement, they used histogram equalization and edge detection to obtain the Region of Interest (ROI). For classification, they used SVM and KNN classifiers to classify the feature vector with results of 91.40% and 88.90%, respectively [6]. Aditya et al. presented a CNN-based method in 2022 that identified and categorized Alopecia Areata from typical camera hair images with 92% accuracy [14]. In 2023, C. Saraswathi and B. Pushpa proposed using Faster Residual Convolutional Neural Network (FRCNN) for Alopecia Areata detection and classification, achieving 84.30% accuracy, and later used a modified extreme learning machine (MELM) to reach 92.64% accuracy [1],[15]. A summary of techniques for detecting and classifying Alopecia Areata using camera images is given in Table 1.

In 2025, Zaib-un-Nisa et al. conducted research on the detection and classification of skin cancer through extensive experiments using a convolutional neural network (CNN). The paper explains that by adding layers, making each Conv2D layer have multiple filters, and removing the dropout layers, significantly improves the classifiers' accuracy from 62.5% to 85% [22]. Moreover, recent advancements in deep learning have led to significant enhancements in medical imaging. Sarwar et al. applied the method of training the Hybrid ResUNET model for skin lesion classification and ACO to bring together computational reliability and clinical adaptation [23].

In 2023, Akram et al. applied combined datasets including histopathological images and several magnification levels to classify breast cancer. The method involves the conversion of histopathological images from Red Green Blue (RGB) to Chrominance to blue and chrominance of red (YCBCR), and image classification through Extreme Gradient Boosting [24]. Ayub et al. proposed a data-driven approach for image detection using a conventional neural network (CNN) for anomaly detection and multilevel deep learning for encoding high-dimensional input data [25]. Sarwar et al. focused on the integration of few-shot learning (FSL) and transfer learning (TL) to enhance the accuracy level and efficiency of classification and imaging detection of breast cancer. These models are trained and compared with F1 score, recall, and the area under the ROC curve (AUC) [26].

1.2 Contribution

The above literature indicates that detecting Alopecia Areata using Dermatoscopic images requires sophisticated equipment and expertise to operate it. However, it is less expensive and easier to manage the detection of Alopecia Areata using camera images, but it lacks accuracy. Therefore, accuracy needs to be improved by using publicly available datasets like the Dermnet dataset, which is mostly used in research to identify Alopecia Areata.

In this paper, we have achieved a higher accuracy of 96.43% by combining Haralick texture features, Hu-moment shape features, and color features for the early detection and classification of Alopecia Areata using camera images. The technique is compared with the related research in the Results and Discussion section. The goal is to develop a reliable diagnostic tool that can assist in the early detection and classification of this chronic condition.

2. Materials and Methods

2.1 Datasets Used

The images are taken from two different datasets to train the framework for the detection of alopecia areata. Images of healthy hair come from the Figaro1k dataset, which consists of a total of 811 images [27]. Whereas, the images of patients' hair are taken from the Dermnet dataset, which contains images of 23 different dermatological conditions, and specifically, 71 images of Alopecia Areata. [28]. A few samples are given in Figure 2. We utilize data augmentation techniques to solve the issue of overfitting when training complex models with small datasets. By creating synthetic samples from the existing training data, these techniques improve the generalization ability of the model. In this work, we employ standard augmentation methods for performance improvement, often cited in the literature [29]. Although there are numerous approaches to create new images from existing training samples, we focus on the most common techniques: rotation, horizontal mirroring, and vertical mirroring. Following the application of augmentation, we end up with a total of 994 images of Alopecia Areata.



Figure 2: Figaro 1k Dataset sample images of healthy hair [27] (a), Dermnet Dataset sample images of Alopecia Areata [28] (b)

2.2 Proposed Methodology

This section discusses the proposed methodology for the detection and classification of Alopecia Areata. Figure 3 provides a visual representation of the proposed model's operation, providing the user with a clear understanding of its internal processes.

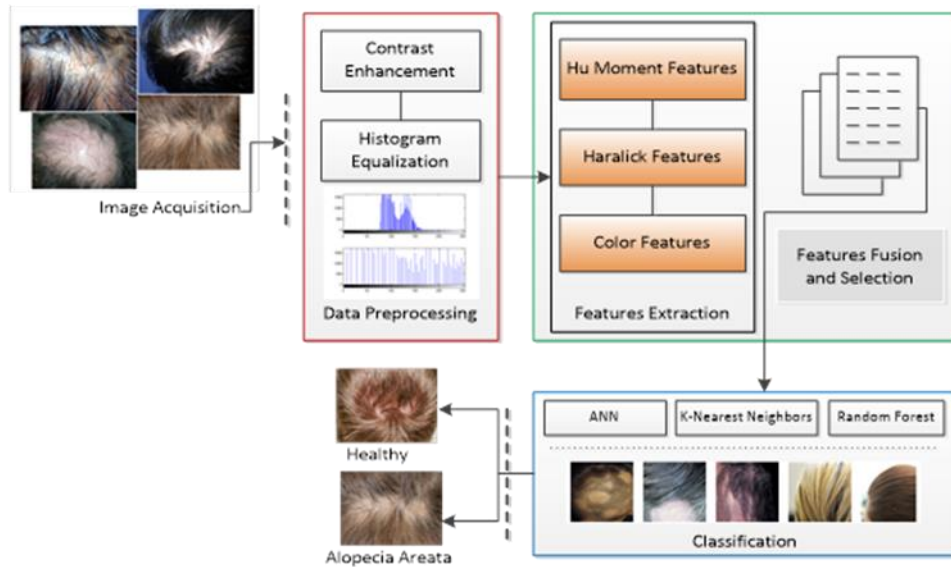


Figure 3: Proposed Methodology

2.3 Preprocessing

Image enhancement aims to enhance the quality of images for certain uses by emphasizing important information and removing unnecessary details from the image [30]. In this study, histogram equalization is employed to enhance the contrast of images. It is considered one of the key methods in image processing. This technique improves an image's contrast and increases its dynamic range by altering its pixel values. The resultant image boasts a more uniform distribution of gray levels due to the rearrangement of pixel intensities, leading to enhanced contrast and visual appeal [31]. In this research, the original color image is converted to grayscale. This transition simplifies the image to various shades of gray, facilitating easier manipulation. Histogram equalization is subsequently applied to modify the brightness levels of the grayscale image. This process improves the image's contrast and uncovers additional details, rendering it clearer and more appropriate for in-depth analysis.

2.4 Feature Extraction

In this research, three primary characteristics are derived from images: texture, shape, and color. Haralick texture features are employed to analyze the textures and patterns present in the images. The hu-moment descriptor is applied to capture shape characteristics such as symmetry and orientation. A color histogram is used to extract color features, allowing for the quantification of color distribution within the images. The fusion of Haralick, Hu-moment, and color histogram features leverages complementary strengths. Haralick captures texture, Hu moments capture shape, and color histograms capture color distribution. This multi-feature approach enriches the representation of image content, leading to better discrimination between classes. As a result, it not only boosts accuracy but also enhances the model's robustness and generalization compared to single-feature methods.

a. Haralick Texture Feature

The technique known as Haralick features enables the extraction of texture information from images by utilizing a gray-level co-occurrence matrix (GLCM). These features serve to statistically represent the arrangement of pixel values within an image. The Haralick texture features offer insights into the textural characteristics of an image [32].

This method is commonly applied in various fields for image interpretation and analysis. The process consists of two phases: calculating and deriving texture features based on the GLCM. The number of gray levels, N_g , defines its

size, which takes the form of a square matrix. The values in this matrix are established by counting the instances where a pixel with value i is adjacent to a pixel with value j , and then normalizing this count by the total number of comparisons made in the matrix. Each element reflects the likelihood that a pixel with value i will be positioned next to a pixel with value j .

Equations (1) to (13) are computed using a co-occurrence matrix to characterize the texture. [32]:

$$Ang\ Sec\ Moment = \sum_i \sum_j Prob(i, j)^2 \quad (1)$$

$$Cont = \sum_{n=0}^{Ng-1} n^2 \left[\sum_{i=1}^{Ng} \sum_{j=1}^{Ng} Prob(i, j) \right], |i - j| = n \quad (2)$$

$$Co\ Rel = \frac{\sum_i \sum_j (ij) prob(i, j) - \mu_x \mu_y}{\sigma_x \sigma_y} \quad (3)$$

$$Var = \sum_i \sum_j (i - \mu)^2 prob(i, j) \quad (4)$$

$$InvDiffMethod = \sum_i \sum_j \frac{1}{1+(i-j)^2} prob(i, j) \quad (5)$$

$$SumAvg = \sum_{i=2}^{2Ng} i Prob_{x+y}(i) \quad (6)$$

$$SumVar = \sum_{i=2}^{2Ng} (i - f_s)^2 Prob_{x+y}(i) \quad (7)$$

$$SumEnt = \sum_{i=2}^{2Ng} Prob_{x+y}(i) \log\{Prob_{x+y}(i)\} = f_s \quad (8)$$

$$Ent = - \sum_i \sum_j Prob(i, j) \log(Prob(i, j)) \quad (9)$$

$$DiffVar = \sum_{i=0}^{Ng-1} i^2 (i) Prob_{x-y}(i) \quad (10)$$

$$DiffEnt = \sum_{i=0}^{Ng-1} Prob_{x-y}(i) \log\{Prob_{x-y}(i)\} \quad (11)$$

$$InfoCo\ Rel\ 1 = \frac{HXY - HXY1}{\max\{HX, HY\}} \quad (12)$$

$$InfoCo\ Rel\ 2 = (1 - \exp[-2(HXY2 - HXY)])^{\frac{1}{2}} \quad (13)$$

b. Hu-Moment Shape Feature

An effective and consistent way to describe important shape features is by using the Hu moment invariant as a feature descriptor, and by its analysis, researchers can extract useful information about a shape's geometry. This information is then useful for a variety of image processing and computer vision tasks, including shape matching, classification, and recognition [33].

Image moments represent the weighted averages of pixel intensities. A mathematical equation can be used to express the image moments for the image $Img(x, y)$, which Moment $_{ij}$ represents.

$$Moment_{ij} = \sum_i \sum_j img(x, y) \quad (14)$$

Equation (14) is used to calculate the pixel intensities. Instead of weighting pixels according to their position, we could assume that they can be weighted according to their intensities. When an image is binary, the quantity of white pixels or regions inside the image is known as the moment. Two similar forms must have the same visual

moments; however, this is an insufficient method. Even though the two images seem to be different, they can both represent the same moment. Equation (15) yields raw image moments that closely resemble central moments.

$$C_{ij} = \sum_x \sum_y (x - \bar{x})^i (y - \bar{y})^j \text{img}(x, y) \quad (15)$$

Central Moments facilitates scale invariance, translation, and rotation. Moments are a set of seven shape features that are independent of image variations and are computed using central moments. The size, rotation, reflection, and translation of the first six moments are invariant. The seventh moment's indicator will change with image reflection [33]. The following

$$m_0 = n_{20} + n_{02} \quad (16)$$

$$m_1 = (n_{20} + n_{02}) + 4n_{11}^2 \quad (17)$$

$$m_2 = (n_{30} + 3n_{12})^2 + (3n_{21} - n_{03})^2 \quad (18)$$

$$m_3 = (n_{30} + n_{12})^2 + (n_{21} + n_{03})^2 \quad (19)$$

$$m_4 = (n_{30} - 3n_{12})(n_{30} + n_{12})[(n_{30} + n_{12})^2 - 3(n_{12} + n_{03})^2] + (3n_{21} + n_{03})[3(n_{30} + n_{12})^2 + (n_{21} + n_{03})^2] \quad (20)$$

$$m_5 = (n_{20} - n_{02})[(n_{30} + n_{12})^2 - (n_{21} + n_{03})^2] + 4n_{11}(n_{30} + n_{12})(n_{21} + n_{03}) \quad (21)$$

$$m_6 = (3n_{21} - n_{03})(n_{30} + n_{12})[(n_{30} + n_{12})^2 - 3(n_{21} + n_{03})^2] + (n_{30} - 3n_{12})(n_{21} + n_{03})[3(n_{30} + n_{12})^2 - (n_{21} + n_{03})^2] \quad (22)$$

c. Color Histogram

The Color Histogram shows the Distribution of color intensities in an image. They facilitate actions like image categorization and retrieval by offering insights into the image's prominent colors, color contrast, and overall color composition [34].

Principal Component Analysis (PCA) is a commonly used technique for data analysis, particularly helpful for applications like data compression, feature extraction, dimensionality reduction, and data visualization [35]. In this study, we have applied this technique on the feature vector after feature fusion to determine the most significant components that contribute to the data's variability. This step is important for classification and recognition.

2.5 Classification

In this study, Random Forest, SVM, Decision Tree, Logistic Regression, Naive Bayes, ANN, and KNN have been utilized for the classification of healthy and Alopecia Areata images into their accurate classes.

Algorithm

Algorithm: An algorithm for the Early detection and classification of Alopecia Areata using Feature Fusion

Input: Scalp image.

Output: Alopecia Areata/Healthy.

1. Read the image.
 2. Apply Histogram Equalization for image enhancement.
 3. Apply Haralick, Hu-Moment, and Color Histogram for texture, shape, and color features, respectively
 4. Apply fusion of the above features
 5. Apply feature selection by using PCA
 6. Apply different classifiers for Alopecia Areata Classification
-

3. Results and Discussion

This section offers detailed insights into the experimental results of the proposed method, along with a thorough discussion of the details provided.

3.1 Experimental Setup

All the experiments are conducted in Python using Google Collab with the images uploaded on Google Drive and categorized into healthy and alopecia areata. After features extraction, the dataset is split into a 7:3 ratio, allocating 70% for training and 30% for testing. To assess the performance of classifiers, Precision, Recall, F1-Score, Accuracy, and Error Rate have been computed for Random Forest, SVM, Decision Tree, Logistic Regression, Naive Bayes, ANN, and KNN classifiers. Finally, the proposed approach is compared with current techniques to show its efficiency.

3.2 Evaluation Metric

For the performance evaluation, Precision, Recall, F1-Score, Accuracy, and Error Rate metrics were calculated. Accuracy metric used to express the performance of a classification model and defined as the percentage of instances that are properly classified. It can be calculated by using Equ. (23).

$$Accuracy = \frac{TN+TP}{TN+FN+FP+TP} \quad (23)$$

True Positive (TP) + False Positive (FP) is a precision metric, which shows us how well we are identifying a class out of all the classes that are predicted as positive classes. It can be calculated by using Equ. (24).

$$Precision = \frac{TP}{FP+TP} \quad (24)$$

The performance of seven different classifiers, namely Random Forest, SVM, Decision Tree, Logistic Regression, Naive Bayes, ANN, and KNN, is evaluated using a confusion matrix. The confusion matrix shows the expected outcomes for the two classes. The true class indicates alopecia areata, while the false class represents healthy hair. When both the actual and predicted values are true, the result is a true positive (TP); otherwise, it results in a false negative (FN). Conversely, when the actual and predicted values are false, the outcome is a true negative (TN); otherwise, it results in a false positive (FP).

For the sake of simplicity, we are showing only one confusion matrix for the ANN classifier, as shown in Figure 4. It represents the higher values of the true negative rate (TNR) of 98.54% and True positive rate (TPR) of 94.19%; on the other hand, both False Negative Rate (FNR) and False Positive Rate (FPR) are low. Overall, it achieved the highest accuracy of 96.43%

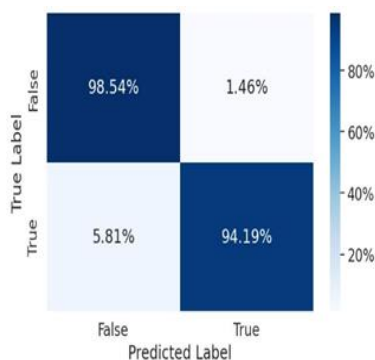


Figure 4: Confusion Matrix of using ANN

The performance and classification results for all seven classifiers are shown in Table 2 **Error! Reference source not found.**

Table 2: Performance metrics summary using different classifiers

Classifier	Class	Precision (%)	Recall (%)	F1-Score (%)	Accuracy (%)
Random Forest	Alopecia Areata	92.10	93.71	92.89	92.29
	Healthy	92.53	90.65	91.58	
Decision Tree	Alopecia Areata	90.07	91.96	91.00	90.23
	Healthy	90.42	88.21	89.30	
SVM	Alopecia Areata	89.81	67.83	77.29	78.57
	Healthy	70.89	91.06	79.72	
GNB	Alopecia Areata	57.95	93.01	71.41	59.96
	Healthy	72.60	21.54	33.23	
Logistic Regression	Alopecia Areata	67.35	80.77	73.45	68.61
	Healthy	70.90	54.47	61.61	
KNN	Alopecia Areata	88.68	98.60	93.38	92.48
	Healthy	98.13	85.37	91.30	
ANN	Alopecia Areata	94.74	98.54	96.60	96.43
	Healthy	98.38	94.19	96.24	

Moreover, the True Positive Rate (TPR) and True Negative Rate (TNR) are high, and on the other hand, False Positive Rate (FPR) and False Negative Rate (FNR) are low, as shown in Table 3.

Table 3: Classification performance using different classifiers

Classifier	TPR (%)	TNR (%)	FPR (%)	FNR (%)	Error rate (%)
Random Forest	91.00	94.00	6.00	9.00	7.71
Decision Tree	88.00	92.00	8.00	12.00	9.77
SVM	91.00	68.00	32.00	9.00	21.43
GNB	22.00	93.00	7.00	78.00	40.04
Logistic Regression	54.00	81.00	19.00	46.00	31.39
KNN	85.00	99.00	1.00	15.00	7.52
ANN	94.00	99.00	1.00	6.00	3.57

The results highlight the outstanding efficacy of the suggested approach employing the ANN classifier, which utilizes the Adam optimizer with a standard learning rate of 0.001 and a batch size of 64, and four layers with ReLU as the activation function Figure 5 and Figure 6 Show training and testing accuracy and loss, respectively. Similarly, Figure 7 shows the ROC curve.

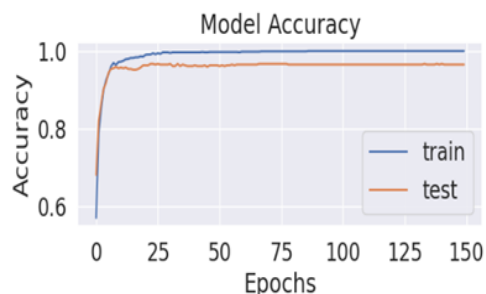


Figure 5: ROC curve showing Model Accuracy

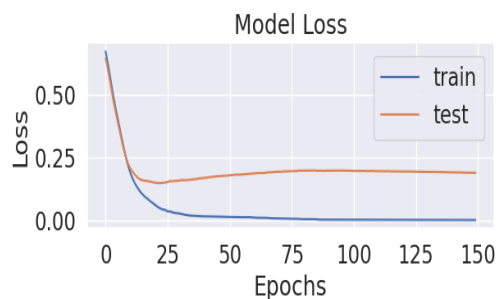


Figure 6: ROC curve showing Model Loss

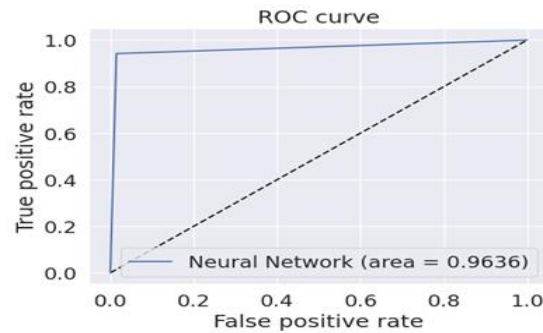


Figure 7: ROC Curve using ANN for FP and TP rates.

3.3 Impact on Classification Accuracy Without Pre-Processing

To further emphasize the importance of preprocessing, Additional results are obtained using the ANN classifier without applying any preprocessing method. The result indicates a significant drop in accuracy, highlighting the importance of preprocessing in improving classification performance.

Figure 8 Illustrates the confusion matrix for the ANN classifier without pre-processing. This matrix reveals a significant drop in both the true negative rate (TNR) and true positive rate (TPR), resulting in an overall accuracy of 92.62%. This accuracy is significantly lower than the results obtained by preprocessing.

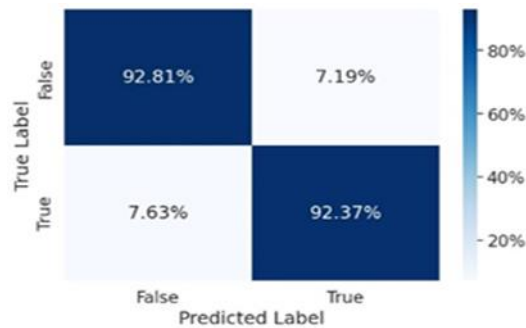


Figure 8: Confusion Matrix of ANN without Pre-processing

3.4 Impact of Different Feature-Set on Classification Accuracy

For the evaluation of the impact of each feature extraction method. The performance of the ANN classifier is evaluated using individual features, their two combinations, and a complete feature fusion approach.

The results, presented in Table 4 Show the classification accuracy achieved with each feature set, its combinations, and the contribution of each feature extraction method. The proposed method, which utilizes feature fusion of all extracted features followed by Principal Component Analysis (PCA), demonstrates the highest accuracy among all methods.

Table 4: Classification Accuracy Comparison by Feature Set

ANN Classifier	Class	Prec. (%)	Recall (%)	F1-Score (%)	Acc (%)
Without Pre-processing	Alopecia Areata	94.04	92.81	93.42	92.62
	Healthy	90.83	92.37	91.60	
With Haralick Texture Features	Alopecia Areata	89.97	89.37	89.67	88.56
	Healthy	86.83	87.55	87.19	
With Hu-Moment shape features	Alopecia Areata	94.37	90.76	92.53	91.51
	Healthy	87.92	92.54	90.17	
With color features using the Color histogram	Alopecia Areata	94.60	91.00	92.77	92.44
	Healthy	90.15	94.07	92.07	
With Haralick and Color Histogram	Alopecia Areata	96.21	93.94	95.06	94.65
	Healthy	92.86	95.51	94.16	
With Haralick and Hu-moment	Alopecia Areata	92.47	92.47	92.47	92.25
	Healthy	92.02	92.02	92.02	
With Hu-Moment and Color Histogram	Alopecia Areata	96.86	92.98	94.88	94.46
	Healthy	91.76	96.30	93.98	
Without Applying PCA	Alopecia Areata	93.93	99.66	96.71	96.31
	Healthy	99.56	92.31	95.80	
Proposed Methodology	Alopecia Areata	94.74	98.54	96.60	96.43
	Areata Healthy	98.38	94.19	96.24	

3.5 Comparison with Related Research

In this section, we compare our findings with the related research that has employed camera images for Alopecia Areata Detection. This focused comparison ensures that our analysis is directly comparable to approaches using similar data sources, providing a clear benchmark for assessing the efficacy and advancements of our approach.

Table 5 It is a comprehensive comparison of our approach to established techniques. It encompasses important factors like the year of publication, the classifier employed, the feature extraction methods, and the accuracy achieved. The same evaluation metrics as those used for computed accuracy are employed, and the same datasets as those used by Figaro1K and Dermnet are utilized by all the researchers mentioned in Table 5. By examining these elements, we can demonstrate the advantages and enhancements of our method compared to others.

Table 5: Comparative Analysis of Alopecia Areata Detection Techniques Using Camera Images

Ref	Year	Dataset	Feature Extraction Technique	Classifier	Acc (%)
[6]	2021	Figaro1K, Dermnet	Shape, Color, and Texture features	SVM	91.40
[20]	2022	Figaro1K, Dermnet	CNN	CNN	92.00
[21]	2023	Dermnet	FRCNN	FRCNN	84.30
[1]	2023	Dermnet	Shape, Color, and Texture features	MELM	92.64
Proposed Method	2024	Figaro1K Dermnet	Haralick texture features, Hu-Moment shape features, and color features	ANN	96.43

4. Conclusion

In this research, we utilized a method for detecting and classifying Alopecia Areata through camera images by focusing on the processes of extracting features, fusing them, and classifying the results. Our study involved the fusion of Color, Hu-moment shape, and Haralick texture features, resulting in a significant improvement in detection accuracy. We evaluated various classifiers, such as Support Vector Machines (SVM), Artificial Neural Networks (ANN), and Random Forest, for their effectiveness, with the proposed approach outperforming current advanced methods.

5. Recommendations for Future Work

For future studies, the strength of the method could be enhanced by employing a larger and more diverse dataset. In addition, combining camera images with other diagnostic tools like dermoscopy or medical imaging might further improve the system's accuracy and dependability.

6. Acknowledgements

This work is supported by the University of Engineering and Technology, Taxila 47050, Pakistan.

7. References

1. Saraswathi, C. and B. Pushpa, *Machine Learning Algorithm for Classification of Alopecia Areata from Human Scalp Hair Images*. Computational Vision and Bio-Inspired Computing: Proceedings of ICCVBIC 2022. 2023: Springer. 269-288.
2. Lintzeri, D.A., et al., *Alopecia areata – Current understanding and management*. J Deutsche Derma Gesell, 2022. **20**(1): p. 59-90.
3. Darwin, E., et al., *Alopecia areata: Review of epidemiology, clinical features, pathogenesis, and new treatment options*. Int J Trichol, 2018. **10**(2): p. 51.
4. Kumar, V.B., S.S. Kumar, and V. Saboo. *Dermatological disease detection using image processing and machine learning*. in *2016 Third International Conference on Artificial Intelligence and Pattern Recognition (AIPR)*. 2016. Lodz: IEEE.
5. Inc., A.A.A.F., *Types Of Alopecia Areata*. Australia Alopecia Areata Foundation, 2025.

6. Shakeel, C.S., et al., *Classification Framework for Healthy Hairs and Alopecia Areata: A Machine Learning (ML) Approach*. Computational and Mathematical Methods in Medicine, 2021. **2021**: p. 1-10.
7. Inui, S., et al., *Clinical significance of dermoscopy in alopecia areata: analysis of 300 cases*. Int J Dermatology, 2008. **47**(7): p. 688-693.
8. C, S. and P. B, *Computer Imaging of Alopecia Areata and Scalp Detection: A Survey*. IJETT, 2022. **70**(8): p. 347-358.
9. Olsen, E. and D. Canfield, *A new take on the severity of alopecia tool (SALT) for determining percentage scalp hair loss*. 2016. **75**(6).
10. Bernardis, E. and L. Castelo-Soccio, *Quantifying Alopecia Areata via Texture Analysis to Automate the SALT Score Computation*. Journal of Investigative Dermatology Symposium Proceedings, 2018. **19**(1): p. S34-S40.
11. Lee, S., *Clinically Applicable Deep Learning Framework for Measurement of the Extent of Hair Loss in Patients With Alopecia Areata*. JAMA Dermatol, 2020. **156**(9): p. 1018.
12. Kapoor, I. and A. Mishra, *Automated Classification Method for Early Diagnosis of Alopecia Using Machine Learning*. Procedia Computer Science, 2018. **132**: p. 437-443.
13. Seo, S. and J. Park, *Trichoscopy of Alopecia Areata: Hair Loss Feature Extraction and Computation Using Grid Line Selection and Eigenvalue*. Computational and Mathematical Methods in Medicine, 2020. **2020**: p. 1-9.
14. Aditya, S., S. Sidhu, and M. Kanchana. *Prediction of Alopecia Areata using Machine Learning Techniques*. in *2022 IEEE International Conference on Data Science and Information System (ICDSIS)*. 2022. IEEE.
15. Saraswathi, C. and B. Pushpa. *FRCNN based Deep Learning for Identification and Classification of Alopecia Areata*. in *2023 Fifth International Conference on Electrical, Computer and Communication Technologies (ICECCT)*. 2023. IEEE.
16. Hung, P.K., et al., *Quantitative assessment of female pattern hair loss*. 2015. **33**(3): p. 142-145.
17. Ludwig, E., *Classification of the types of androgenetic alopecia (common baldness) occurring in the female sex*. Br J Dermatol, 1977. **97**(3): p. 247-254.
18. Savin, R., *A method for visually describing and quantitating hair loss in male pattern baldness*. Journal of Investigative Dermatology, 1992. **98**: p. 604.
19. Lee, S.H. and C.S. Yang, *AN INTELLIGENT HAIR AND SCALP ANALYSIS SYSTEM USING CAMERA SENSORS AND NORWOOD-HAMILTON MODEL*. p. 16.
20. Norwood, O.T., *Male Pattern Baldness: classification and Incidence*. Southern Medical Journal, 1975. **68**(11): p. 1359-1365.
21. Benhabiles, H. and et al. *Deep Learning based Detection of Hair Loss Levels from Facial Images*. in *2019 Ninth International Conference on Image Processing Theory, Tools and Applications (IPTA)*. 2019. Istanbul, Turkey: IEEE.
22. Unnisa, Z., et al., *Impact of fine-tuning parameters of convolutional neural network for skin cancer detection*. Scientific reports, 2025. **15**(1): p. 1-23.
23. Sarwar, N., et al., *Skin lesion segmentation using deep learning algorithm with ant colony optimization*. BMC Medical Informatics and Decision Making, 2024. **24**(1): p. 265.
24. Akram, A., et al., *Recognizing Breast Cancer Using Edge-Weighted Texture Features of Histopathology Images*. Computers, Materials & Continua, 2023. **77**(1).
25. Ayub, N., et al., *Forecasting Multi-Level Deep Learning Autoencoder Architecture (MDLAA) for Parametric Prediction based on Convolutional Neural Networks*. Engineering, Technology & Applied Science Research, 2025. **15**(2): p. 21279-21283.

26. Sarwar, N., S. Al-Otaibi, and A. Irshad, *Optimizing Breast Cancer Detection: Integrating Few-Shot and Transfer Learning for Enhanced Accuracy and Efficiency*. International Journal of Imaging Systems and Technology, 2025. **35**(1): p. e70033.
27. *Figaro 1K*. Available from: <https://www.michelesvanera.org/figaro-1k/>.
28. *Dermnet*. Available from: <https://www.kaggle.com/datasets/shubhamgoel27/dermnet>.
29. Inoue, H., *Data Augmentation by Pairing Samples for Images Classification*. 2018.
30. Qi, Y. and et al., *A Comprehensive Overview of Image Enhancement Techniques*. Arch Computat Methods Eng, 2022. **29**(1): p. 583-607.
31. Liangping, T. and D. Changqing. *Histogram equalization and image feature matching*. in *2013 6th International Congress on Image and Signal Processing (CISP)*. 2013. IEEE.
32. Simonthomas, S., N. Thulasi, and P. Asharaf. *Automated diagnosis of glaucoma using Haralick texture features*. in *International conference on information communication and embedded systems (ICICES2014)*. 2014. IEEE.
33. Žunić, J., K. Hirota, and P.L. Rosin, *A Hu moment invariant as a shape circularity measure*. Pattern Recognition, 2010. **43**(1): p. 47-57.
34. Nazir, A., et al. *Content based image retrieval system by using HSV color histogram, discrete wavelet transform, and edge histogram descriptor*. in *2018 International Conference on Computing, Mathematics and Engineering Technologies (iCoMET)*. 2018. Sukkur: IEEE.
35. Takio, K., *Principal component analysis (PCA)*, in *Computer vision: a reference guide*. 2019. p. 1-4.